Biomedicine & Pharmacotherapy 118 (2019) 109232

Contents lists available at ScienceDirect

Biomedicine & Pharmacotherapy

journal homepage: www.elsevier.com/locate/biopha

Triptriolide antagonizes triptolide-induced nephrocyte apoptosis via inhibiting oxidative stress *in vitro* and *in vivo*

Xiao-wan Wang[a,1], Rui-min Tian[a,b,1], Yi-qi Yang[a], Zhao-Yu Lu[a,b], Xiao-dong Han[a,b], Xu-sheng Liu[a,b], Wei Mao[a,b], Peng Xu[b,c,*], Hong-tao Xu[d,**], Bo Liu[a,b,*]

[a] *The Second Clinical Medical College, and Guangdong Provincial Key Laboratory of Clinical Research on Traditional Chinese Medicine Syndrome, Guangzhou University of Chinese Medicine, Guangzhou, 510006, PR China*
[b] *Guangdong Provincial Academy of Chinese Medical Sciences, Guangzhou, 510006, PR China*
[c] *The Second Clinical Medical College, and Guangdong Provincial Key Laboratory of Chinese Medicine for Prevention and Treatment of Refractory Chronic Diseases, Guangzhou University of Chinese Medicine, Guangzhou, 510006, PR China*
[d] *Shanghai Institute for Advanced Immunochemical Studies, ShanghaiTech University, Shanghai, 201210, PR China*

ARTICLE INFO

Keywords:
Triptriolide
Triptolide
Oxidative stress
Apoptosis
Nrf2 pathway

ABSTRACT

Triptolide(T9) is a predominant bioactive component extracted from Chinese herb *Tripterygium wilfordii Hook F.* (TwHF), and has multiple pharmacological activities, such as immunosuppressive and anti-inflammatory activities, et al. However, severe adverse effects and toxicity, particularly nephrotoxicity, limit its clinical application. It has been demonstrated that the activation of nuclear factor erythroid 2-related factor 2 (Nrf2) signaling pathway could alleviate T9-induced nephrocyte damage. The aim of this study was to investigate the potential protective role of triptriolide (T11) against T9-induced nephrocyte apoptosis *in vitro* and *in vivo*. Renal injury models were established in human kidney 2 (HK2) cells and BALB/c mice using T9, and the protective effects of T11 were probed *in vitro* and *in vivo*, respectively. T9 induced nephrocyte damage in HK2 cells and BALB/c mice by induction of reactive oxygen species (ROS), lactate dehydrogenase (LDH), malondialdehyde (MDA) and glutathione (GSH) and reduction of superoxide dismutase (SOD), which resulted in the apoptosis of nephrocyte and injury of renal function. While, pretreatment of T11 effectively reversed these changes, resulting in the obvious decrease of oxidative stress and renal function parameters, ameliorated nephrocyte apoptosis, improved cell morphology, and higher increase of Nrf2, NAD(P)H: quinine oxidoreductase 1 (NQO1) and heme oxygenase 1 (HO-1) protein levels *in vitro* and *in vivo*. Altogether, T11 protected against T9-induced nephrocyte apoptosis possibly *via* suppressing oxidative stress.

1. Introduction

Tripterygium wilfordii Hook F. (TwHF) is a well-known traditional Chinese herbal medicine that has been widely used for the therapy of autoimmune diseases, including nephritic syndrome, systemic lupus erythematosus, and rheumatoid arthritis [1]. Triptolide (T9), the major bioactive component of TwHF, possesses various promising pharmacological effects of TwHF [2]. However, the clinical development of T9 has been hindered greatly due to its severe side effects to digestive, blood circulatory, urinary, reproductive, immune systems as well as bone marrow [3], and particularly, its severe toxicity to the kidney [4].

Oxidative stress, induced by harmful stimulus, can damage all cellular macromolecules, including proteins, lipids, and DNA [5]. Uncontrolled production of oxidants results in oxidative stress that impairs cellular functions and contributes to the development of cellular injury [6]. Moreover, oxidative stress caused by the dysfunction of mitochondrial, the inhibition of lysosomal hydrolase, phospholipid injury, and increased intracellular calcium concentration could directly lead to drug-induced nephrocyte injury [7]. Accumulated studies have shown that oxidative stress products and lipid peroxidation were detected in T9-treated rats, indicating that oxidative stress played a vital role in T9-induced cytotoxicity to kidney [8]. Oxidative stress is closely related to cell apoptosis in some diseases [9–11]. What's more, published study has demonstrated that reactive oxygen species (ROS) plays an important role in T9-induced apoptosis of renal tubular cells and renal injury [12].

* Corresponding authors at: Guangdong Provincial Academy of Chinese Medical Sciences, Guangzhou, 510006, PR China.
** Corresponding author.
E-mail addresses: xupeng@gzucm.edu.cn (P. Xu), xuht@shanghaitech.edu.cn (H.-t. Xu), doctliu@263.net, doctliu@gzucm.edu.cn (B. Liu).
[1] These authors contributed equally to this paper.

https://doi.org/10.1016/j.biopha.2019.109232
Received 17 June 2019; Received in revised form 14 July 2019; Accepted 15 July 2019

The cellular defense system governs a series of cytoprotective genes to counteract oxidative stress. Nuclear factor erythroid 2-related factor 2 (Nrf2) is one of most famous family members for its primary cytoprotective role in response to oxidative and electrophilic stress [13]. Nrf2 regulates specifically genes embodying anti-oxidative elements (ARE), including xenobiotic-metabolizing, and cytoprotective enzymes [14]. Under normal conditions, Nrf2 is inhibited retaining in the cytosol by Kelch-like ECH-associated protein 1 (Keap1), which functions as a negative regulator of Nrf2 by binding to Nrf2 to promote ubiquitination and enhancing its proteasomal degradation [15]. However, under the condition of exposing to ROS and electrophiles, Nrf2 disaggregates from Keap1 and accumulates into the nucleus where it dimerizes with members of small Maf proteins [16], binds to ARE, and ultimately activates ARE-dependent gene expression, including NAD(P)H: quinine oxidoreductase 1 (NQO1) and heme oxygenase 1 (HO-1) [17]. The Nrf2 pathway forms a pivotal node in cellular protective system against oxidative and electrophilic stresses from both exogenous and endogenous origins, resulting in reversing cell apoptosis.

Triptriolide (T11), an active diterpene component which is similar to T9, was obtained from Chinese herb medicine TwHF and has had a great impact on attenuation synergia of TwHF. Our previous studies have shown that T11 could be a potent agent to relieve hepatocyte injury induced by lipopolysaccharide (LPS) *in vivo* and *in vitro* [18]. In addition, the prominent protective effect of T11 on puromycin aminonucleoside (PAN)-induced podocyte injury has been elucidated [19]. However, there is no indication on the impact of T11 on T9-induced oxidative stress-mediated renal apoptosis *in vitro* and *in vivo* to date.

The present study aims to explore the potential protective effects of T11 against T9-induced renal oxidative stress-mediated apoptosis in human kidney 2 (HK2) cells and BALB/c mice. The current results provide empirical evidence for the anti-oxidative activity of T11 *via* Nrf2 signaling pathway and the antagonistic effect of T11 on T9-induced oxidative stress-associated renal apoptosis, and allow further insight into the therapeutic schedules against T9-induced side effect to kidney.

2. Materials and methods

2.1. Chemicals and reagents

T11, purity > 98%, was obtained from Liubo laboratory (Guangzhou, China). T9 purity > 98%, was obtained from Nanjing Dilger Medical Technology Co., Ltd (Nanjing, China). Dimethyl sulfoxide (DMSO) was purchased from Sigma-Aldrich (St. Louis, MO, United States). 3-(4,5-Dimethylthiazol-2-yl)-2,5-diphenyl-tetrazolium bromide (MTT) was purchased from MP Biomedicals (Santa Ana, CA, USA). Phosphate buffer saline (PBS), Hanks' Balanced Salt Solution (HBSS), Dulbecco's modified Eagle's medium (DMEM/F12), Fetal bovine serum (FBS) and 0.25% Trypsin-EDTA were purchased from GIBCO Laboratories (Grand Island, NY, United States). Annexin V-FITC/PI apoptosis kit was obtained from MultiSciences (Hangzhou, China). TUNEL apoptosis assay kit was purchased from Beyotime Biotechnology Institution (Jiangsu, Nanjing). 4′,6-Diamidino-2-phenylindole (DAPI) was purchased from Sigma-Aldrich (St. Louis, MO, USA). Primary antibodies against Nrf2 (#12721), Keap1 (#8407) and GAPDH (#5174) were purchased from Cell Signaling Technology Inc. (Beverly, MA, United States). Primary antibodies against HO-1 (ab13248), NQO1 (ab28947) were purchased from ABCAM (Abcam, Cambridge, MS, United States). SuperSignal West Femto Maximum Sensitivity Substrate was obtained from Thermo Fisher Scientific Inc. (Rockford, IL, United States). ROS test kit was purchased from Beyotime Biotechnology (Shanghai, China). Other reagents were of analytical grade from commercial suppliers.

2.2. Cell culture and MTT assay

The human renal proximal tubular cell line HK2 cells, obtained from Chinese Academy of Sciences Cell Bank (Shanghai, China), were cultured in DMEM/F12 supplemented with 10% (v/v) FBS. The cells were grown in a humidified 37 ℃ incubator with 5% CO_2. T9 and T11 were dissolved in DMSO and stock solutions were stored at -20℃. Reagents were freshly diluted to the marked concentrations with culture medium before use. DMSO concentration in experimental conditions never exceeded 0.1%(v/v).

Cell viability was detected using MTT assay kit. HK2 cells were seeded in a 96-well cell plate (9×10^3 cells/well). The HK2 cells were treated with T9 (0, 5, 10, 20, 40, 80, 160, 320, 640 nM) or T11 (0, 0.0625, 0.125, 0.25, 0.5, 1, 2, 4 mM) for 24 h. MTT (5 mg/mL, 20 μL/well) were added 24 h later and the cells were incubated for another 4 h. The violet formazan precipitate in cells was dissolved with DMSO (150 μL/well). Following shaking for 5 min, the absorbance of solubilized formazan grains in HK2 cells was measured at 490 nm. Next, HK2 cells were seeded in a 96-well cell culture plate (9×10^3 cells/well) and then treated with the selected concentration of T9 (50 nM) with T11 (0, 0.25, 0.5, 0.75, 1 mM) for 24 h. The MTT assay was removed, DMSO was added and the absorbance was measured. Finally, HK2 cells (2.7×10^5cells/well) were seeded into a 6-well cell culture plate and treated with T9 (50 nM) for 24 h with or without selected concentration of T11 (0.5 mM), and morphological changes of cells were observed and captured by microscope (Olympus BX53, Japan).

2.3. Annexin V-FITC/PI staining by flow cytometric analysis

HK2 cell apoptosis from each group was detected by flow cytometry using the Annexin V-FITC/PI Apoptosis Detection Kit according to the manufacturer's instructions. As shown in Fig. S1, HK2 cells (2.7×10^5 cells/well) were seeded in a 6-well culture plate and treated with T9 (50 nM) with or without T11 (0.5 mM) for 24 h. Then the cells were collected by centrifugation at 1500 rpm for 5 min and washed twice with pro-cooling PBS. Following resuspending with 500 μL Binding Buffer, the cells were stained by Annexin V-FITC solution (5 μL) and PI solution (10 μL). The cells were vortexed softly and incubated at room temperature for 5 min in dark. The Annexin V-FITC/PI positive cells were analyzed by flow cytometry (BD). Approximately 1×10^4 cells from each group were gated and counted, and the distribution ratios of early apoptotic cells (Q3: lower right quadrant) and late apoptotic cells (Q2: upper right quadrant) were calculated for comparison between groups.

2.4. Release of LDH leakage in HK2 cells

The leakage of Lactate dehydrogenase (LDH) from the cells was assessed by CytoTox 96 Non-Radioactive Cytotoxicity Assay (Promega, Madison, USA) as the manufacturer described. Briefly, HK2 cells were seeded in a 96-well culture plate at a density of 9×10^3 cells/well and treated by T9 (50 nM) with or without T11 (0.5 mM) for 24 h. And 50 μL supernatant of the cells were removed in a new 96-well culture plate. 50 μL CytoTox were added and incubated at room temperature in dark for 30 min. After adding with 50 μL Stop Solution, the cells were measured at 490 nm using microplate reader (Biotek Gen5, USA).

2.5. Oxidative stress indicators in HK2 cells

The cells were treated with T9 (50 nM) for 24 h with or without T11 (0.5 mM) when plated in 96-well culture plates at a suitable density (9×10^3 cells/well). After treatment, the HK2 cell supernatant was used to detect oxidative stress indicators including malondialdehyde (MDA), superoxide dismutase (SOD), glutathione (GSH), and cell extracts prepared in RIPA buffer (CWBIO, Beijing, China) containing Proteinase inhibitor Tablets (Roche, Mannheim, Germany) were used to

detect relative protein levels.

2.6. Animals and experimental protocol

The specific-pathogen-free (SPF) healthy male BALB/c mice, 6–8 weeks old, weighing 18–22 g, were purchased from Laboratory Animal Services Center, Guangzhou University of Chinese Medicine (Guangzhou, China). The mice were housed in an animal room, and under environment condition with controlled temperature (20 ± 2 °C), humidity (50 ± 10%), a 12 h light/dark cycle (lights on: 07:00-19:00), ventilation, more than 10 air exchanges per hour (all-fresh-air system) and had free access to a standard diet and water *ad libitum*. Experimental protocols were inspected and permitted by Animal Care and Use Committee (Guangzhou university of Chinese medicine, Guangzhou).

As shown in Fig. S2, 18 mice were randomly assigned to 3 groups (n = 6 per group): 1) control; 2) T9 (1 mg/kg); 3) T11 (28 mg/kg) + T9. The dosage of T11 was selected according to our previous study [18]. And the dosage of T9 was selected refer to the published article [8]. T11 was administered *via* oral gavage, while T9 was injected by intraperitoneally (i.p.). The mice were received T11 once daily by gavage for 7 days consecutively. T9 was given to establish acute kidney injury animal model after the final treatment of T11. After 24 h, all animals were anesthetized and required samples were collected. Serum samples were collected for biochemical analysis. And kidney tissues were removed and weighed. The sections of the kidney were collected for analysis of biochemistry and protein expression and staining of immunohistochemical and TUNEL.

2.7. Evaluation of kidney coefficient in mice

All BALB/c mice were weighed before anesthetized. Kidney tissues were collected and weighed immediately after sacrificed, the kidney coefficient was measured by the formula [20] (1):

$$\text{The kidney coefficient}(\%) = \frac{Wk}{Wb} \times 100\% \quad (1)$$

where *Wk* and *Wb* represent the kidney weight and body weight, respectively.

2.8. Serum Cr and BUN activities

The serum creatinine (Cr) and blood urea nitrogen (BUN) levels were used as sensitive indicators of kidney injury. The measurement of Cr and BUN was performed as previously described [21]. Briefly, blood samples in each group were collected and let stand for 1 h. Serum samples were obtained by centrifuging blood samples at 3000 rpm for 15 min. The concentrations of Cr and BUN in serum were detected by assay kits (Siemens, India) and analyzed with auto analyzer (Siemens, Dimension Xpand^{plus}, USA).

2.9. Oxidative stress indicators in renal tissues

Renal tissues of 50 mg were homogenized in 800 μL PBS and centrifuged at 12,000 rpm for 15 min at 4 °C. Then the supernatants were removed for oxidative stress indicators assay. The levels of MDA, SOD, GSH and LDH were measured to assess oxidative stress in each group. All the above indicators were conducted using corresponding assay kit (Nanjing Jiancheng Bioengineering Institute, Nanjing, China) refer to the protocol's instructions.

2.10. Determination of ROS production

The production of ROS in kidney sections was measured by a fluorescent probe 2′,7′-Dichlorodi-hydrofluorescein diacetate (DCFH-DA, Beyotime Biotechnology, China) according to the procedure previous reported with a few modifications [22]. The kidney portions were collected and washed gently with PBS, and then diverted into a culture dish containing 5 mL PBS. Put the kidney tissues on 200 mesh filter and gently crush the kidney tissues with syringe core to obtain cell suspensions. Then the cell suspensions were collected in centrifugal tube and centrifuged at 500 × g for 5 min. After discarding supernatant, adding1 × erythrocyte lysate to resuspend precipitation, reaction in dark at room temperature for 10 min, neutralized with equal volume PBS, centrifuged at 500 × g for 5 min. After discarding the supernatant, then resuspended nephrocytes with 3 ml PBS and counted. The nephrocytes (9×10^3 cells/well) were plated in a 96-well culture plate and stained with DCFH-DA (10 μM) for 30 min at 37 °C. The fluorescent intensity was determined at an excitation wavelength of 488 nm and emission wavelength of 525 nm.

2.11. Western Blot

Western Blot was performed as previously described with a few adjustments [23]. Total proteins were extracted from kidney tissues or HK2 cells using RIPA lysis buffer (CWBIO, Beijing, China) with Proteinase inhibitor Cocktail Tablets (Roche, Mannheim, Germany) according to the protocol. After centrifuging the collected solutions at 12,000 rpm for 15 min, the supernatant was removed and added by loading buffer, then the mixture was boiled for 10 min. Equivalent amounts of proteins were loaded and split by 10% SDS-polyacrylamide gel electrophoresis and transferred to PVDF membranes (Millipore Co, Billerica, MA, United States). The bands were blocked in 5% nonfat milk in TBST for 2 h at room temperature and then incubated overnight at 4 °C with corresponding primary antibodies. The bands were then incubated with a secondary antibody conjugated with horseradish peroxidase at 37 °C in moist chamber for 2 h. The membranes were developed using SuperSignal West Femto Maximum Sensitivity Substrate (Thermo Fisher Scientific, Rockford, IL, United States) according to the manufacturer's protocol. The immunoreactive density were detected by a chemiluminescence detection system (Bio-Rad Laboratories, Hercules, CA, United States). The bands were analyzed using Image Lab software 5.2.1(Bio-Rad Laboratories, Hercules, CA, United States).

2.12. TUNEL staining

After apoptosis, the genomic DNA in the nucleus breaks. With the catalysis of Terminal Deoxynucleotidyl Transferase (TdT), exposed 3′-OH can bind with fluorescent probe Cy3 labeled dUTP, which can be detected by fluorescence confocal microscopy. Apoptosis DNA fragmentation in kidney tissue was measured by TUNEL assay kit (C1089, Biotime Institute) as previously described with a few adjustments [24]. Briefly, kidney sections (3 μm) from each group were dewaxed. Following incubation with protease K (without DNase, 20 μg/mL) for 30 min at 37 °C. After washing with PBS, the sections were incubated with 50 μL TUNEL reaction mixture for 60 min at 37 °C in dark. Subsequently, stained sections were washed with PBS and observed by fluorescence confocal microscope (Zeiss LSM710, Germany). The number of the TUNEL positive cells was calculated in 10 randomly selected fields of 6 sections by Image J (Bio-Rad Laboratories, Hercules, CA, United States) for comparison.

2.13. Immunohistochemical staining

Immunohistochemical studies for mice kidney slices were performed to detect the expression and location of Nrf2 as described previously with a few modifications [25]. 4% paraformaldehyde-fixed, paraffin-embedded kidney tissues (3 μm) were dewaxed initially. 3% hydrogen peroxide (H_2O_2) was added to block the activity of endogenous peroxidase for 15 min. Kidney sections from different groups were washed twice using PBS. Following incubation in 1% Triton-X 100 solution for 30 min at room temperature, and then antigen retrieval

with citric acid buffer (pH 6.0) in microwave. And subsequently a blocking solution containing 3% bovine serum albumin (BSA) was added to block for 30 min at room temperature. Kidney slices were stained with anti-Nrf2 antibody (1:200 dilution) in a moist chamber for 2 h at 37 ℃. After washing three times with PBS buffer solution, the secondary antibody was added. Then the kidney samples were incubated in a moist chamber at 37 ℃for 1 h and washed with PBS buffer solution before addition with 3, 3′-Diaminobenzidine (DAB) (Maxim Biotechnology Development Co., Ltd., China) for 5 s. Nuclei were counterstained by hematoxylin, dehydration in graded alcohols and stepping in TO (substitute for xylene), mounted by neutral gum. Images were captured by microscope (Olympus BX53, Japan), and six fields were chosen randomly. In addition, the positive expression of IHC was analyzed by Image Lab software 5.2.1.

2.14. Statistical analysis

SPSS 17.0 (SPSS, Inc., Chicago, IL, USA) was used for statistical analysis. Results from the experiments are expressed as mean ± SEM. Two-group comparisons were analyzed using the Student's *t*-test or one-way analysis of variance (ANOVA) followed by Turkey's test when appropriate. Statistical significance was defined as $P < 0.05$. Special Statistical significance was defined as $P < 0.01$.

3. Results

3.1. The structure, high resolution mass spectra, spectrum of T11

The structure of T11 and its high-resolution mass spectra, spectrum of ^{1}H and ^{13}C-NMR were shown in published article [18].

3.2. Effects of T11 and T9 on HK2 cell viability

Treatment of T9 for 24 h impaired the HK2 cell viability in a dosage-dependent manner. T9 50 nM was used in following experiments which was close to the IC_{50} value (Fig. 1A). Treatment with T11 didn't show any cytotoxicity at 0–1 mM, but a dosage-dependent decrease of cell viability at 1–4 mM (Fig. 1B). T11 treatment could significantly ameliorate T9-induced decline of cell viability at 0.25-0.75 mM in a dosage-dependent manner (Fig. 1C). Thus, the middle effective dose (0.5 mM) was selected for subsequent experiments. Besides, T9 treatment could cause HK2 cells to be slender, grow antennae and death, while T11 could counteract those changes (Fig. 1D).

3.3. Effects of T11 and T9 on HK2 cell apoptosis

Annexin V-FITC/PI double staining cell apoptosis detection assay was used to further investigate the effects of T9 and T11 on HK2 cell apoptosis. As shown in Fig. 2, T9 could significantly elevate the early apoptosis of HK2 cells ($P < 0.01$) compared with the control group, while T11 co-treatment could markedly decrease the early apoptosis of HK2 cells ($P < 0.01$) when compared to the T9 treated group. The result of the Annexin V-FITC/PI assay indicated that T11 could protect HK2 cells against T9-induced nephrocyte apoptosis *in vitro*.

3.4. Effects of T11 and T9 on oxidative stress indicators in HK2 cells

To investigate the potential anti-oxidative effect of T11 in T9-induced HK2 nephrocytes, LDH, MDA, SOD and GSH levels were measured in the supernatant of HK2 nephrocytes. As shown in Fig. 3A–D, there were a significant induction of LDH ($P < 0.01$) and MDA ($P < 0.01$) and depletion of SOD ($P < 0.01$) together with GSH ($P < 0.01$) in cells exposed to T9 (50 nM) compared to the control group. In contrast, T11 (0.5 mM) co-treatment markedly lower the concentration of LDH ($P < 0.01$) and MDA ($P < 0.01$), and triggered the rise of SOD ($P < 0.05$) and GSH ($P < 0.01$) compared with T9-treated group.

3.5. Effects of T11 and T9 on Nrf2 pathway activation in HK2 cells

To further determine the changes in the protein levels of Nrf2 signaling pathway after T11 and/or T9 co-treatment, HK2 cells were treated with T11 (0.5 mM) and T9 (50 nM), and the expressions of Nrf2, NQO1, HO-1 and Keap1 were analyzed by Western Blot. As shown in Fig. 4, Nrf2 ($P < 0.01$) protein levels of T9-injured group slightly increased, as well as its downstream NQO1 ($P < 0.01$) and HO-1 ($P < 0.01$) compared with the control group, and further enhanced with the co-treatment of T11 (Fig. 4B–D). Furthermore, Western Blot depicted that the treatment of T9 with or without T11 didn't result in significant change in expression of Keap1 in each group (Fig. 4E).

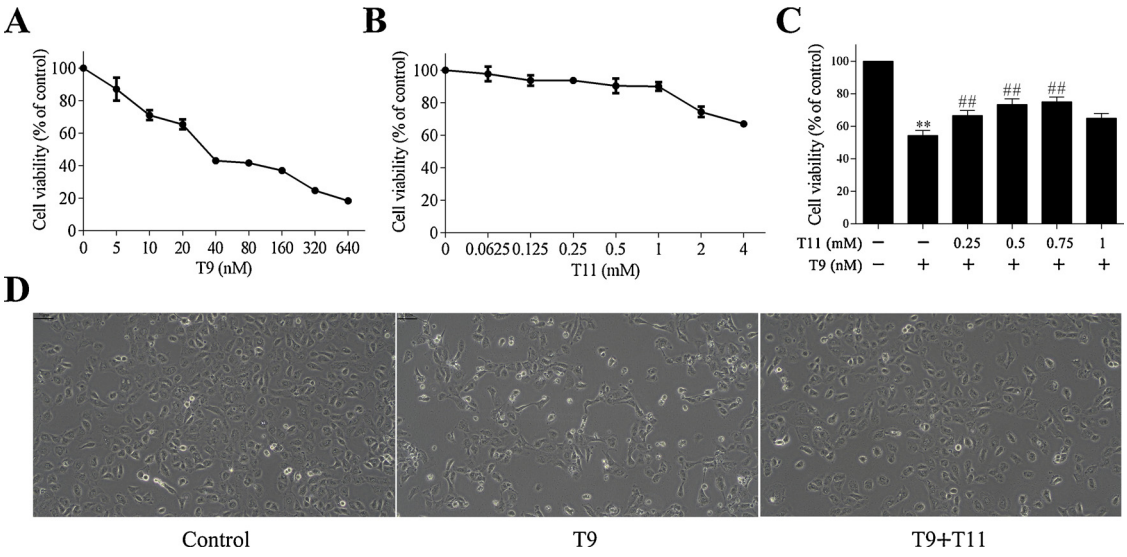

Fig. 1. Effects of T9, T11 and T9 + T11 on the viability and morphological changes of HK2 cells. **A**. HK2 cells were treated with T9 at different concentrations for 24 h. **B**. HK2 cells were treated with T11 at different concentrations for 24 h. **C**. HK2 cells were treated with T9 (50 nM) for 24 h with or without T11 with indicated concentrations. **D**. HK2 cells were treated with T9 (50 nM) for 24 h with or without T11 (0.5 mM), and morphological changes of cells were observed and captured by microscope (magnification × 200). The cell viability was detected by MTT assay kit. Data are represented as the mean ± SEM from independent groups. $^{**}P < 0.01$ *vs.* control group. $^{\#\#}P < 0.01$ *vs.* T9 group.

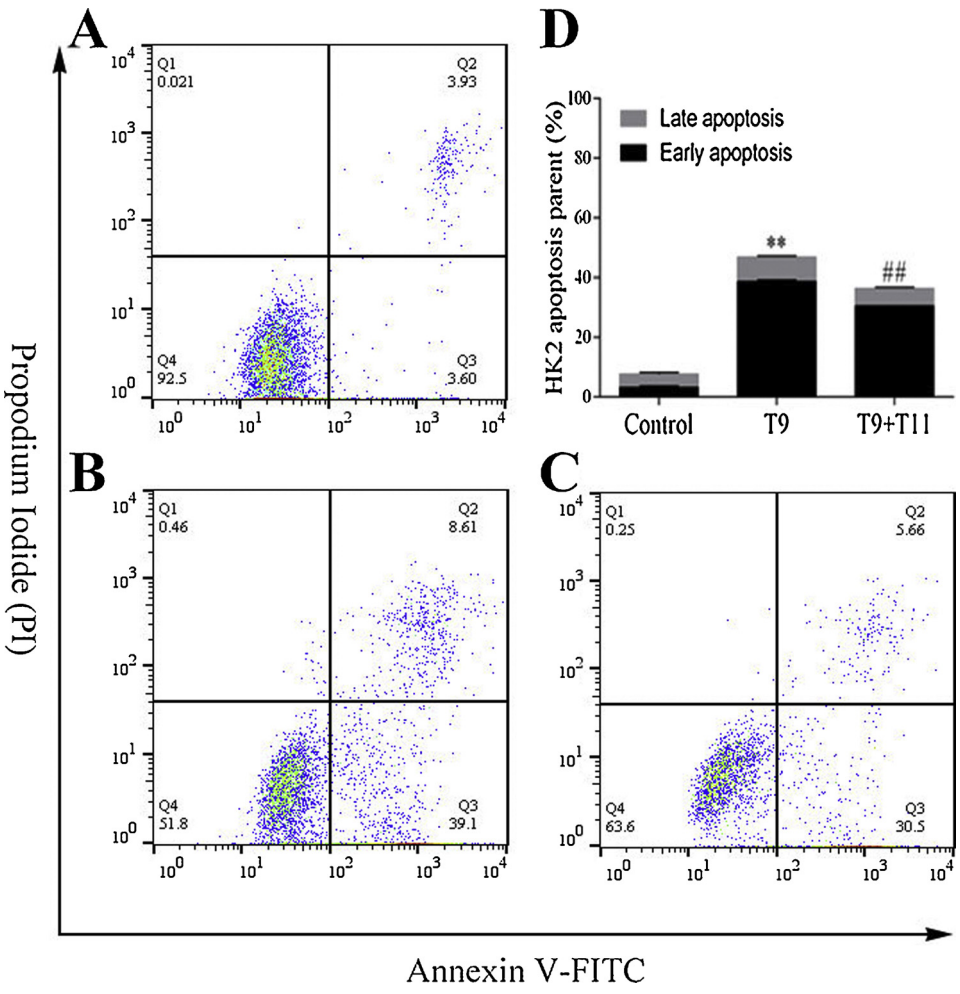

Fig. 2. HK2 cell apoptosis in different groups determined by Annexin V-FITC/PI uptake and flow cytometry detection. HK2 cells were treated with or without T9 (50 nM)/T11 (0.5 mM) for 24 h. The distributions of apoptotic and necrotic cells in the control group (**A.**), the T9 group (50 nM) (**B.**) and the T9 (50 nM) + T11 (0.5 mM) group (**C.**) were detected by Annexin V-FITC/PI double staining assay. And the ratio of apoptotic cell in each group was shown in (**D.**). Q1 (Annexin V-FITC-negative/PI-positive) represents necrotic cells, Q2 (Annexin V-FITC- positive /PI-positive) represents late apoptotic cells, Q3 (Annexin V-FITC-positive/ PI-negative) represents early apoptotic cells, and Q4 (Annexin V-FITC-negative/PI-negative) represents living cells. Data are represented as the mean ± SEM from independent groups. $^{**}P < 0.01$ *vs.* control group. $^{\#\#}P < 0.01$ *vs.* T9 group.

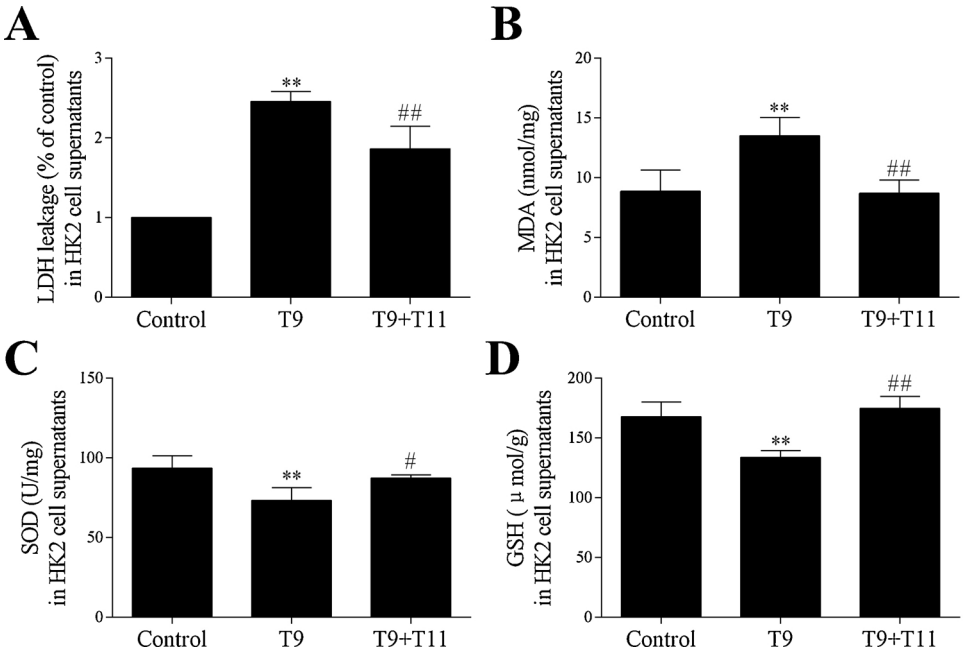

Fig. 3. HK2 cells were treated with T9 (50 nM) for 24 h with or without T11 (0.5 mM), indicators of oxidative stress in cell supernatants were measured. Effects of T9 or T9 + T11 on the levels of LDH (**A**), MDA (**B**), SOD (**C**) and GSH (**D**) in HK2 cell supernatants were detected. Cell supernatants were analyzed by assay kit. Data are represented as the mean ± SEM from independent groups. $^{**}P < 0.01$ *vs.* control group. $^{\#}P < 0.05$, $^{\#\#}P < 0.01$ *vs.* T9 group.

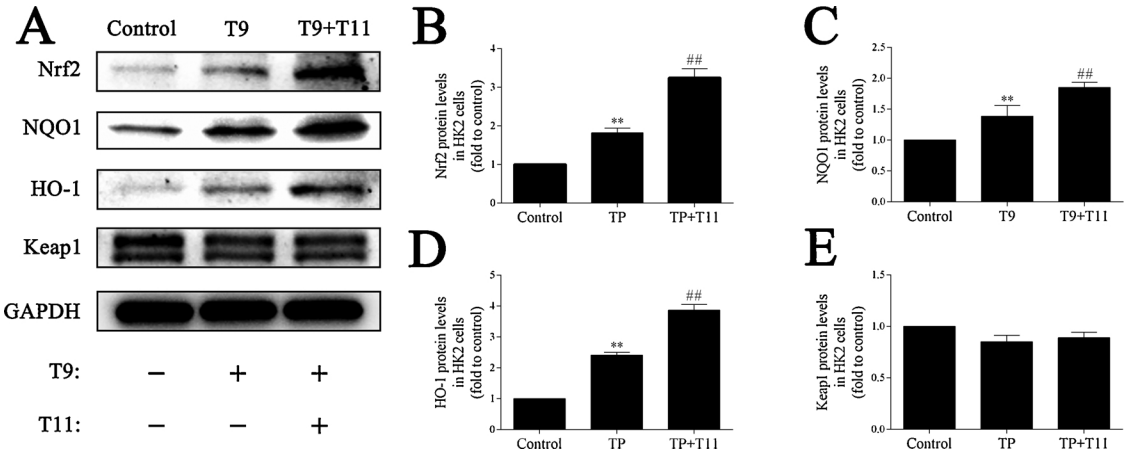

Fig. 4. T11 pretreatment induced the expression levels of Nrf2 pathway in HK2 cells to protect against T9-induced nephrotoxicity. HK2 cells were treated with T9 (50 nM) for 24 h with or without T11 (0.5 mM) pretreatment. **A**. The protein levels of Nrf2, NQO1, HO-1 and Keap1 in each group were measured by Western Blot. **B**. Nrf2 protein expression. **C**. NQO1 protein expression. **D**. HO-1 protein expression. **E**. Keap1 protein expression. Data are represented as the mean ± SEM from independent groups. $^{**}P < 0.01$ *vs*. control group. $^{\#\#}P < 0.01$ *vs*. T9 group.

3.6. Effects of T11 and T9 on kidney coefficient in mice

During our experiment, body weight was recorded every day and kidney tissue was weighed immediately after sacrifice. As shown in Fig. 5A–B, there was no obvious change in body weight and the absolute size of the mice kidney in each group. There was not obvious difference in the kidney coefficient of each group.

3.7. Effects of T11 and T9 on kidney function indicators in mice

Nephrotoxicity was monitored by quantitative analysis of Cr and BUN levels that were used as the biochemical markers of renal injury. The parameter of nephrotoxicity from different groups was shown in Fig. 5E–F. Giving acute single dose of T9 (1 mg/kg), the Cr ($P < 0.01$) and BUN ($P < 0.01$) were significantly elevated compared to the control

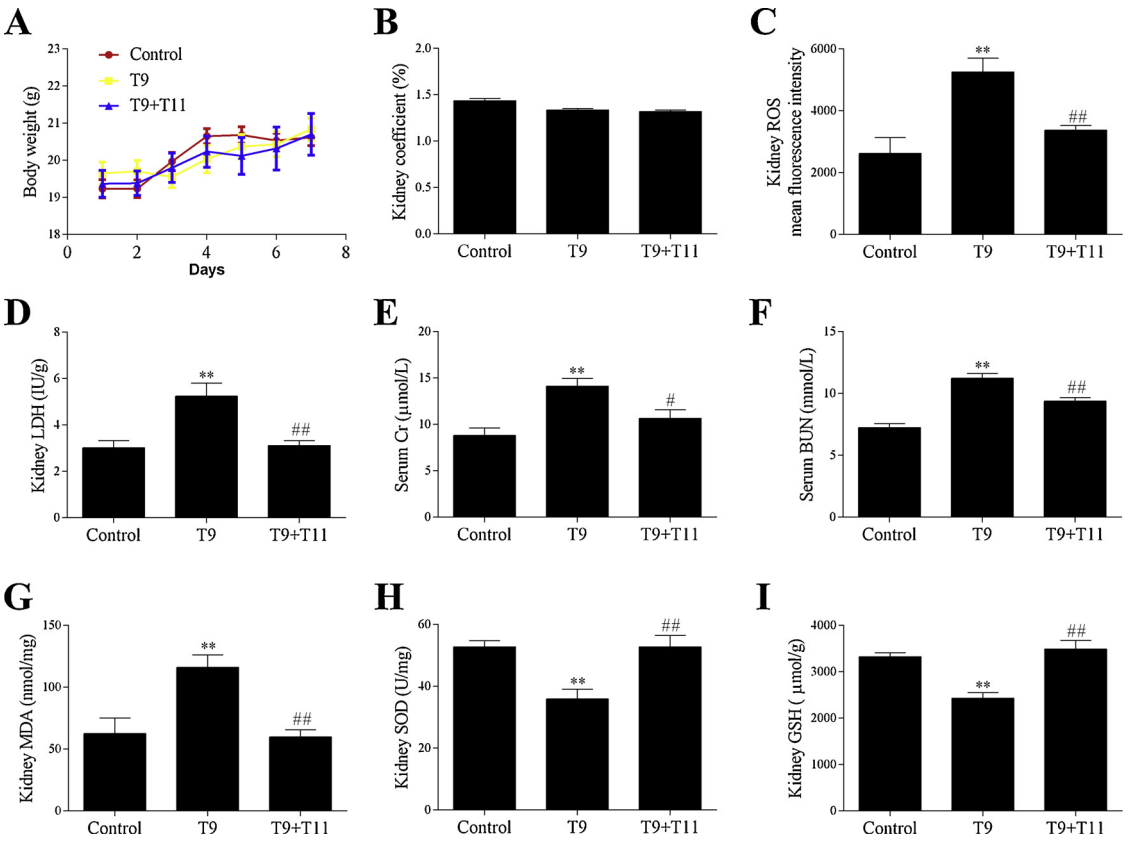

Fig. 5. Effects of T9 and T11 on body weight, kidney coefficient changes and indicators of kidney function and oxidative stress in kidney of BALB/c mice. The mice were received T11 (28 mg/kg) once daily by gavage for 7 days consecutively. T9 (1 mg/kg) was given to establish acute injury animal model after the final treatment of T11. Body weight was measured every day (**A**) and kidney tissues (wet) were weighed after sacrifice and the kidney coefficient (**B**) was calculated. Cr (**E**) and BUN (**F**) in the blood serum of mice were measured after treatment of T11 with or without T9 for 7 days. And oxidative biochemical parameters of ROS (**C**), LDH (**D**), MDA (**G**), SOD (**H**) and GSH (**I**) were detected in kidney tissues. Data are represented as the mean ± SEM from independent groups. $^{**}P < 0.01$ *vs*. control group. $^{\#}P < 0.05$, $^{\#\#}P < 0.01$ *vs*. T9 group.

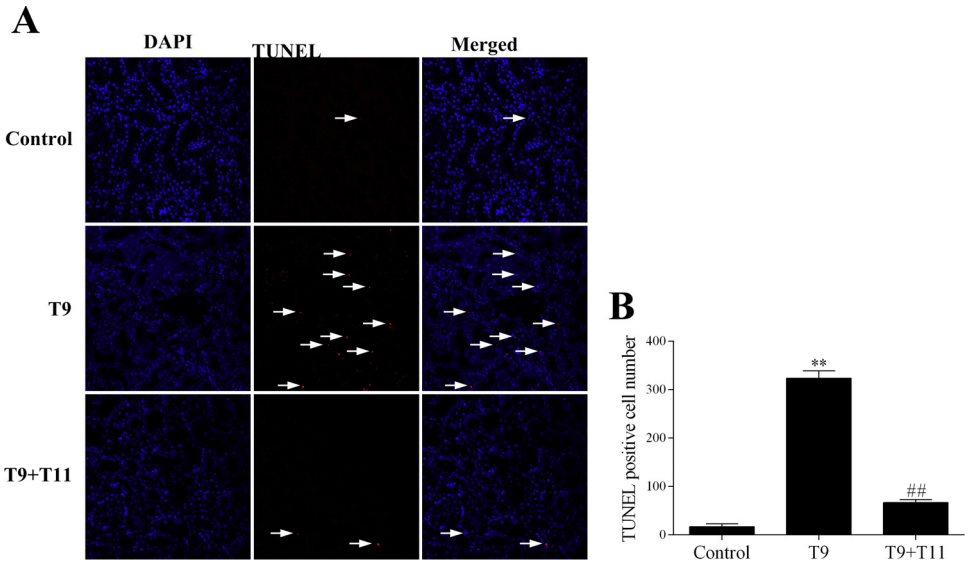

Fig. 6. Kidney paraffin sections were stained by TUNEL assay (red) to detect renal tissue damage and counterstained with DAPI (blue) (magnification × 100, white arrows). **A**. The kidney sections were stained with DAPI dye and labeled with dUTP. **B**. TUNEL positive cell numbers in kidneys of each group.

group. Pretreatment of T11 once daily for 7 days, the Cr ($P < 0.05$) and BUN ($P < 0.01$) levels of the T9 + T11 group in the serum were significantly reduced compared to the T9 group, respectively, indicating that T11 significantly reduced Cr and BUN levels in the serum of BALB/c mice.

3.8. Effects of T11 on T9 on oxidative stress in mice

An animal model of acute kidney injury induced by T9 was established. As shown in Fig. 5C, D, G—I, activities of ROS ($P < 0.01$), LDH ($P < 0.01$) and MDA ($P < 0.01$) in the T9 group were elevated, respectively, when compared with those in the control group. While the levels of SOD ($P < 0.01$) and GSH ($P < 0.01$) were significantly reduced. However, Pretreatment of T11 reduced the increase of ROS ($P < 0.01$), LDH ($P < 0.01$) and MDA ($P < 0.01$), respectively, when compared with the T9 group. While the activities of SOD ($P < 0.01$) and GSH ($P < 0.01$) were increased, when compared to the T9 group.

3.9. Effects of T11 and T9 on nephrocyte apoptosis in mice

During apoptosis, DNA endonucleases are activated, which cut off genomic DNA in the nucleus. Exposed 3′-OH can be dyed red by TUNEL staining reagent. As shown in Fig. 6, the TUNEL positive cell number in T9-treated group was significantly increased ($P < 0.01$), when compared to the control group. While pretreatment of T11 could dramatically reduce the level of TUNEL positive cell, when compared with the T9 treated group. The results of TUNEL assay confirmed that T11 could reverse the apoptosis of renal cells triggered by T9.

3.10. Effects of T11 and T9 on the protein levels of Nrf2 pathway in mice

The total Nrf2 expression was detected in the mouse kidneys by Western Blot. As shown in Fig. 7B, T9 administration triggered the increase of total level of Nrf2 (compared to the control group, $P < 0.01$), moreover, T11 pretreatment elevated much higher expression of total Nrf2 compared with the T9 group ($P < 0.01$).

To confirm the effect of T11 on Nrf2-related downstream targets, we analyzed relative protein levels of kidney tissues by Western Blot. Fig. 7C–E showed that T9 stimulated higher expression of NQO1 ($P < 0.01$) and HO-1 ($P < 0.01$) compared to the control group, and T11 pretreatment caused dramatic increase in NQO1 ($P < 0.01$) and HO-1 ($P < 0.01$) proteins compared to the T9 group. The expression of Keap1 has not been changed much. The result indicated that Nrf2 activation is involved in the protective effect of T11 on T9-induced kidney injury.

3.11. Immunohistochemistry

To determine the location and expression change of Nrf2 protein in kidney tissues of BALB/c mice, immunohistochemistry was implemented on kidney sections from different groups. Photomicrographs of typical fractions were shown in Fig. 8A–D. Treatment of T9 could slightly promote the transfer of Nrf2 to the nucleus compared to the control group. However, pretreatment with T11 stimulated more Nrf2 to transfer to the nucleus. Besides, Nrf2 expression was enhanced higher in T9-treated group than that of the control group, but strong positively expressed in T9 + T11 co-treated BALB/c mice.

4. Discussion

T9 is one of the primary bioactive chemical components of traditional Chinese herbal medicine (TCHM)-*Tripterygium wilfordii Hook F.* (TwHF), which exhibits numerous pharmacological activities, including immunosuppressive, anti-cancer, anti-inflammatory, anti-rheumatoid, anti-osteoporosis, anti-fertility and anti-cystogenesis [26]. Besides, T9 has an obvious protective effect on nephrocytes and could significantly ameliorate kidney pathological damage [27,28]. However, multiple organ toxicity of T9, especially potential nephrotoxicity, challenges its advance for reaching clinic [29]. In the study of attenuation of TwHF, we confirmed T11, a diterpene diepoxide, to exert a considerable impact on amelioration synergia of TwHF. Our previous studies indicated that T11 had a potential protective effect on LPS-induced hepatocyte injury and PAN-induced podocyte injury. In our present study, we employed the human renal proximal tubular HK2 cells and BALB/c mice as experimental models both *in vitro* and *in vivo* to probe the effect of T11 in the resistance to T9-induced oxidative stress-mediated apoptosis of nephrocytes. Our studies showed that T9 was found to trigger apoptosis induced by oxidative stress *in vitro* and *in vivo*, and pre-treatment of T11 exerted attenuation effect in which Nrf2 pathway is concerned.

Oxidative stress has got much attention, in our present study, for its vital role of involving in T9-induced renal injury as verified previously [30]. Oxidative stress induced by T9 in HK2 cells was determined by elevating levels of LDH and MDA and declining levels of SOD and GSH,

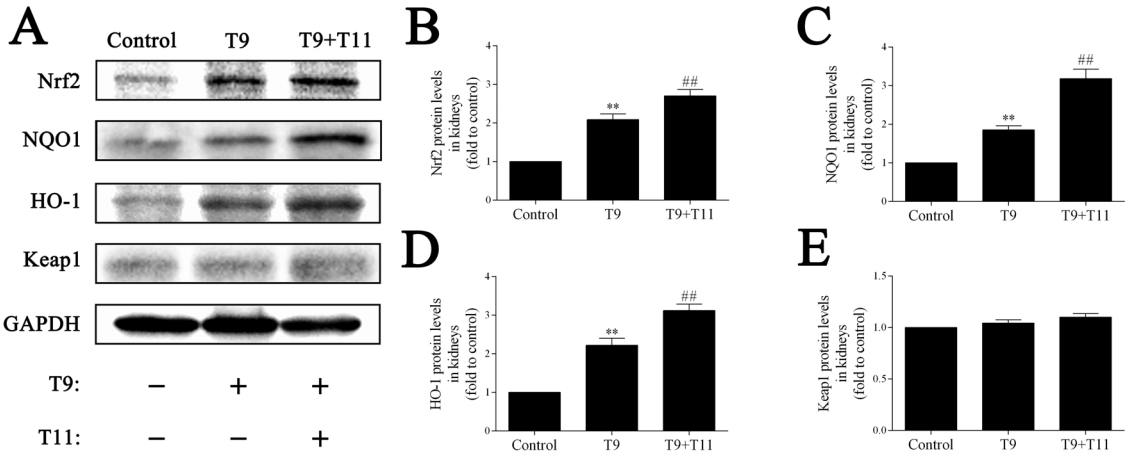

Fig. 7. T11 pretreatment induced the expression levels of Nrf2 pathway in BALB/c mice to protect against T9-induced nephrotoxicity. BALB/c mice were treated with T9 (1 mg/kg) for 24 h with or without T11 (28 mg/kg) pretreatment. **A**. The protein levels of Nrf2, NQO1, HO-1 and Keap1 from each group in kidney of mice were measured by Western Blot. **B**. Nrf2 protein expression. **C**. NQO1 protein expression. **D**. HO-1 protein expression. **E**. Keap1 protein expression. Data are represented as the mean ± SEM from independent groups. $^{**}P < 0.01$ *vs*. control group. $^{\#\#}P < 0.01$ *vs*. T9 group.

however, T11 could reverse this condition in *vitro*. Additionally, an animal drug-induced injury model set up in BALB/c mice was used to assess the effect of T9 and T11 on oxidative stress *in vivo*. Consistent with the results of cell experiment, T9 exposure induced oxidative stress in kidneys of BALB/c mice determined by increasing concentrations of ROS, LDH and MDA, as well as decreasing levels of SOD and GSH as previous reported [8,12]. But pretreatment of T11 could counteract the oxidative stress damage caused by T9 in BALB/c mice.

The excess of ROS can trigger damage to intracellular constituents, including proteins and DNA of the functional systems of organelle, resulting in irreversible cell injury and even apoptosis, which can lead to various of diseases [31]. In this study, we further investigate the nephrocyte injury in HK2 cells and BALB/c mice using flow cytometry and TUNEL staining assay. In order to ascertain HK2 cell apoptosis induced by T9, the Annexin-V-FITC/PI was applied using flow cytometry method. And the results revealed that unlike T9-induced obvious HK2 cell apoptosis, T11 could significantly inhibit the increase of apoptosis cells. The TUNEL assay results also showed that T11 could protect BALB/c kidney against T9-induced apoptosis injury.

Cr is the end product of nitrogen metabolism, which is transported from blood to urine through the kidney [32]. The level of serum Cr is relatively steady, and there is no more than 10–15% of its average during 124 h. Thus, Cr is a more sensitive index of renal function compared to BUN [33]. BUN is measured by the amount of urea

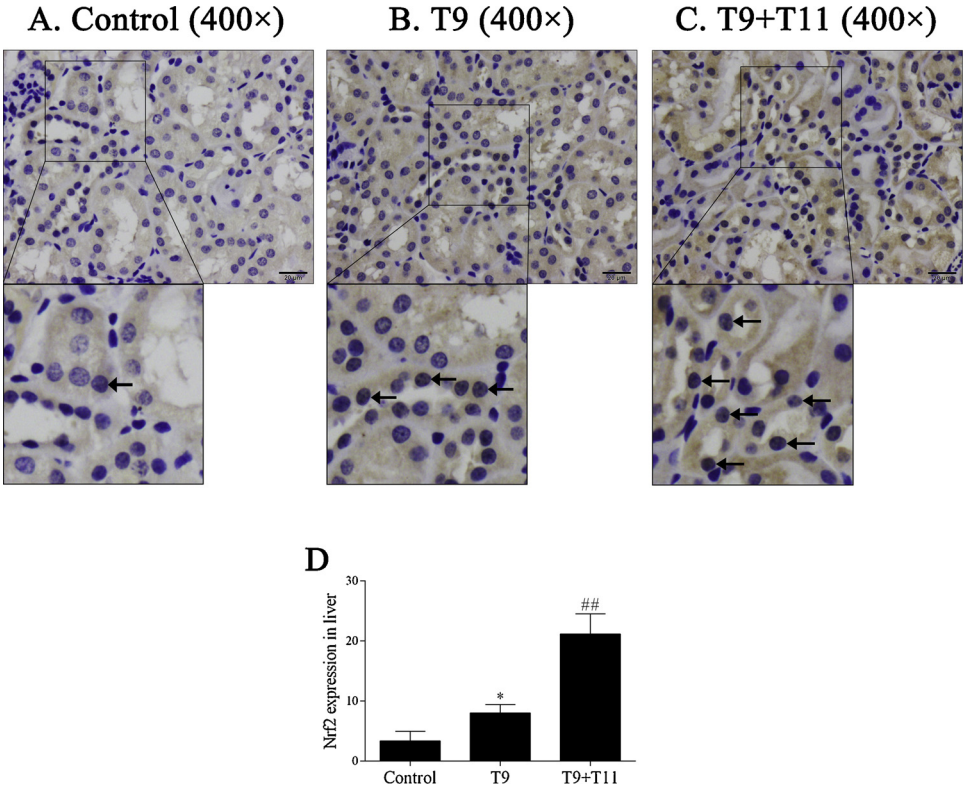

Fig. 8. The immunohistochemical analysis of Nrf2 expression and location in the kidney tissues of BALB/c mice was exerted (magnification × 400, black arrows). **A**. Control. **B**. T9 (1 mg/kg), **C**. T9 (1 mg/kg) +T11 (28 mg/kg). **D**. The expression of Nrf2 in kidney.

nitrogen in the blood, which is the waste of protein metabolism. Detection of BUN residues in blood can be used to evaluate renal function [34]. The changes of Cr and BUN can be used as key indicators of renal function [35]. In our present study, T9-induced kidney injury in BALB/c mice, characterized by increased concentrations of Cr and BUN, was eliminated by pretreatment of T11. In brief, the above results indicated that T11 could alleviate T9-induced nephrocyte apoptosis in which oxidative stress involved *in vitro* and *in vivo*.

We further determined the protein levels of Nrf2 and downstream target proteins including exogenous metabolic enzyme NQO1 and detoxifying enzyme HO-1 by Western Blot. Results from cellular and animal experiments revealed that T11 pretreatment markedly activated the protein expressions of Nrf2 and target proteins, including NQO1 and HO-1, compared to T9 treated group both *in vitro and in vivo* to alleviate oxidative stress damage induced by T9. In addition, the levels of Nrf2 in immunohistochemical analysis is consistent with that of protein expression.

We have attempted to interpret the mechanisms within it. As one of the most important cell protection pathways to maintain homeostasis at the cellular, tissue and organism levels, Nrf2 pathway plays an important part in protection against acute renal injury [36]. Nrf2 is a transcription factor sensing oxidative stress and restoring homeostasis [37]. In the absence of oxidative stress, Nrf2 is isolated in the cytoplasm by bond to the zinc finger protein Keap1, which acts as a substrate receptor for the ubiquitin E3 ligase complex of Cul3-Rbx1. Nrf2 has a high affinity for Keap1 owe to its special functional Neh domains [38]. In the condition of cell damage caused by oxidative stress or electrophilic stress, Nrf2 escapes the inhibition of Keap1 and accumulates in the nucleus, where it dimerizes with small Maf proteins and then ARE, up-regulates downstream target genes including xenobiotic-metabolizing enzyme NQO1 and cytoprotective enzyme HO-1 [39]. NQO1 is widely distributed in organs, but it is highest in liver, kidney and gastrointestinal tract [40]. NQO1 belongs to phase II metabolic enzymes, which together with other phase I and II metabolic enzymes constitute the metabolic network of exogenous toxic substances *in vivo* and play an important role in detoxification metabolism of organisms [41]. In addition, NQO1 participates in antioxidant biological processes and is found to concern stabilization of key regulatory proteins under stress [42]. HO-1 is a cytoprotective enzyme which catalyze the rate-limiting step of heme degradation, thus producing equal molar amounts of iron ions, biliverdin and CO. Biliverdin and bilirubin are formed under the action of biliverdin reductase (BVR). They are effective antioxidants and other products of HO-1 activity regulating biological processes [43]. HO-1 has dual functions of receiving and transmitting by sensing cellular apoptosis and damage and effectively trying to recover intracellular vitality and function [44]. Taken together, the above results indicated that T11 could ameliorate T9-induced renal apoptosis *via* inhibiting oxidative stress.

Remarkedly, the relative protein expressions of Nrf2, NQO1 and HO-1 in T9-treated group were higher than that of the control group. As a main mediator of cellular defense for oxidative/electrophilic signals, the expression of Nrf2 could be elevated as soon as T9 is exposed to the subjects [30]. When T9 causes oxidative stress damage to the kidney tissue, Nrf2 pathway is triggered. Nevertheless, deleterious effects cannot be completely overcome, although adaptively stimulated Nrf2 can alleviate or relieve the toxicity of T9 to nephrocytes. The possible theory is consistent with previous reports [45,46]. Similarly, Activated Nrf2 signaling pathway could protect kidney tissue to some extent, but it was unable to completely counteract the damage of T9 to kidney, so changes were found in serological and biochemical indicators.

Collectively, the present study was to clarify for the first time that the nephroprotective effect of T11 against T9-induced apoptosis associated with oxidative stress may be related to the activation of Nrf2 signaling pathway by T11 *in vitro* and *in vivo*. And these results suggested that T11 might be a choice to prevent T9-induced renal injury and a potent Nrf2 agonist. In the follow-up works, we will further explore the antagonistic effect of T11 on chronic kidney injury induced by T9 and relative mechanisms involved.

5. Conclusions

T11 could protect against T9-induced nephrocyte apoptosis by conquering oxidative stress through activating Nrf2 pathway *in vitro* and *in vivo*, indicating the protecting effect of T11 in treatment of T9-induced renal injuries and the agonizing effect of T11 in Nrf2 signaling pathway. Additionally, it provides novel remedy to counteract the toxicity of T9.

Funding

This work was financially supported by the National Key Research and Development Program of China (No. 2018YFC1707900); the National Natural Science Foundation of China (Nos. 81774216, 81202398 and 81873261); the Specific Research Project of State Administration of TCM of China (No. JDZX2015207); Guangdong Provincial Science and Technology Project (Nos. 2014A020221035, 2015A020211025, 2017B030314166 and 2018B030322012); Guangzhou Science and Technology Project (No. 201607010338); Special Funds for Inheriting and Developing the Traditional Chinese Medicine from TCM Bureau of Guangdong Province (Nos. 20191137 and 20191142); the Specific Research Fund for TCM Science and Technology of Guangdong Provincial Hospital of Chinese Medicine (Nos. YN2016QJ05, YN2016QJ08 and YN2015MS03); and the Key Project of First-class University Construction of Guangzhou University of Chinese Medicine (Nos. XK2018019 and XK2019023).

Declaration of Competing Interest

The authors declare that there are no conflicts of interest.

Appendix A. Supplementary data

Supplementary material related to this article can be found, in the online version, at doi:https://doi.org/10.1016/j.biopha.2019.109232.

References

[1] Y. Zhao, Y. Zhang, P. Su, J. Yang, L. Huang, W. Gao, Genetic transformation system for woody plant Tripterygium wilfordii and its application to product natural celastrol, Front. Plant Sci. 8 (2017) 2221.
[2] X.Y. Li, S.S. Wang, Z. Han, F. Han, Y.P. Chang, Y. Yang, M. Xue, B. Sun, L.M. Chen, Triptolide restores autophagy to alleviate diabetic renal fibrosis through the miR-141-3p/PTEN/Akt/mTOR pathway, Mol. Ther. Nucleic Acids 9 (2017) 48–56.
[3] L. Zhang, J. Chang, Y. Zhao, H. Xu, T. Wang, Q. Li, L. Xing, J. Huang, Y. Wang, Q. Liang, Fabrication of a triptolide-loaded and poly-gamma-glutamic acid-based amphiphilic nanoparticle for the treatment of rheumatoid arthritis, Int. J. Nanomedicine 13 (2018) 2051–2064.
[4] X. Li, et al., Triptolide: progress on research in pharmacodynamics and toxicology, J. Ethnopharmacol. 155 (1) (2014) 67–79.
[5] S.E. Lacher, J.S. Lee, X. Wang, M.R. Campbell, D.A. Bell, M. Slattery, Beyond antioxidant genes in the ancient Nrf2 regulatory network, Free Radic. Biol. Med. 88 (Pt B) (2015) 452–465.
[6] Q. Ma, Role of nrf2 in oxidative stress and toxicity, Annu. Rev. Pharmacol. Toxicol. 53 (2013) 401–426.
[7] K. Hosohata, Role of oxidative stress in drug-induced kidney injury, Int. J. Mol. Sci. 17 (11) (2016).
[8] F. Yang, L. Ren, L. Zhuo, S. Ananda, L. Liu, Involvement of oxidative stress in the mechanism of triptolide-induced acute nephrotoxicity in rats, Exp. Toxicol. Pathol. 64 (7-8) (2012) 905–911.
[9] E. Radi, P. Formichi, C. Battisti, A. Federico, Apoptosis and oxidative stress in neurodegenerative diseases, J. Alzheimers Dis. 42 (Suppl. 3) (2014) S125–52.
[10] R. He, M. Cui, H. Lin, L. Zhao, J. Wang, S. Chen, Z. Shao, Melatonin resists oxidative stress-induced apoptosis in nucleus pulposus cells, Life Sci. 199 (2018) 122–130.
[11] D. Wu, Q. Hu, X. Liu, L. Pan, Q. Xiong, Y.Z. Zhu, Hydrogen sulfide protects against apoptosis under oxidative stress through SIRT1 pathway in H9c2 cardiomyocytes, Nitric Oxide 46 (2015) 204–212.
[12] F. Yang, L. Zhuo, S. Ananda, T. Sun, S. Li, L. Liu, Role of reactive oxygen species in triptolide-induced apoptosis of renal tubular cells and renal injury in rats, J. Huazhong Univ. Sci. Technol. Med. Sci. 31 (3) (2011) 335–341.

[13] P. Canning, F.J. Sorrell, A.N. Bullock, Structural basis of Keap1 interactions with Nrf2, Free Radic. Biol. Med. 88 (2015) 101–107.
[14] D. Cheng, R. Wu, Y. Guo, A.N. Kong, Regulation of Keap1-Nrf2 signaling: the role of epigenetics, Curr. Opin. Toxicol. 1 (2016) 134–138.
[15] C. Tonelli, I.I.C. Chio, D.A. Tuveson, Transcriptional regulation by Nrf2, Antioxid. Redox Signal. 29 (17) (2018) 1727–1745.
[16] M. Yamamoto, T.W. Kensler, H. Motohashi, The KEAP1-NRF2 system: a thiol-based sensor-effector apparatus for maintaining redox homeostasis, Physiol. Rev. 98 (3) (2018) 1169–1203.
[17] P. Deshmukh, S. Unni, G. Krishnappa, B. Padmanabhan, The Keap1-Nrf2 pathway: promising therapeutic target to counteract ROS-mediated damage in cancers and neurodegenerative diseases, Biophys. Rev. 9 (1) (2017) 41–56.
[18] Y.Q. Yang, X.T. Yan, K. Wang, R.M. Tian, Z.Y. Lu, L.L. Wu, H.T. Xu, Y.S. Wu, X.S. Liu, W. Mao, P. Xu, B. Liu, Triptriolide alleviates lipopolysaccharide-induced liver injury by Nrf2 and NF-kappaB signaling pathways, Front. Pharmacol. 9 (2018) 999.
[19] Y.-q. Yang, J. Liang, X.-d. Han, R.-m. Tian, X.-s. Liu, W. Mao, H.-t. Xu, B. Liu, P. Xu, Dual-function of triptriolide in podocytes injury: inhibiting of apoptosis and restoring of survival, Biomed. Pharmacother. 109 (2019) 1932–1939.
[20] H. Zhao, J. Hong, X. Yu, X. Zhao, L. Sheng, Y. Ze, X. Sang, S. Gui, Q. Sun, L. Wang, F. Hong, Oxidative stress in the kidney injury of mice following exposure to lanthanides trichloride, Chemosphere 93 (6) (2013) 875–884.
[21] S.M. Mir, H.G. Ravuri, R.K. Pradhan, S. Narra, J.M. Kumar, M. Kuncha, S. Kanjilal, R. Sistla, Ferulic acid protects lipopolysaccharide-induced acute kidney injury by suppressing inflammatory events and upregulating antioxidant defenses in Balb/c mice, Biomed. Pharmacother. 100 (2018) 304–315.
[22] Y. Lian, X. Xia, H. Zhao, Y. Zhu, The potential of chrysophanol in protecting against high fat-induced cardiac injury through Nrf2-regulated anti-inflammation, antioxidant and anti-fibrosis in Nrf2 knockout mice, Biomed. Pharmacother. 93 (2017) 1175–1189.
[23] I. Arany, S. Hall, D.K. Reed, C.T. Reed, M. Dixit, Nicotine enhances high-fat diet-induced oxidative stress in the kidney, Nicotine Tob. Res. 18 (7) (2016) 1628–1634.
[24] L. Xia, Q. Huang, D. Nie, J. Shi, M. Gong, B. Wu, P. Gong, L. Zhao, H. Zuo, S. Ju, J. Chen, W. Shi, PAX3 is overexpressed in human glioblastomas and critically regulates the tumorigenicity of glioma cells, Brain Res. 1521 (2013) 68–78.
[25] L. Liu, M.K. Vollmer, A.S. Ahmad, V.M. Fernandez, H. Kim, S. Dore, Pretreatment with Korean red ginseng or dimethyl fumarate attenuates reactive gliosis and confers sustained neuroprotection against cerebral hypoxic-ischemic damage by an Nrf2-dependent mechanism, Free Radic. Biol. Med. 131 (2019) 98–114.
[26] H. Xu, B. Liu, Triptolide-targeted delivery methods, Eur. J. Med. Chem. 164 (2019) 342–351.
[27] Y. Hong, W. Zhou, K. Li, S.H. Sacks, Triptolide is a potent suppressant of C3, CD40 and B7h expression in activated human proximal tubular epithelial cells, Kidney Int. 62 (4) (2002) 1291–1300.
[28] M. Xue, Y. Cheng, F. Han, Y. Chang, Y. Yang, X. Li, L. Chen, Y. Lu, B. Sun, L. Chen, Triptolide attenuates renal tubular epithelial-mesenchymal transition via the MiR-188-5p-mediated PI3K/AKT pathway in diabetic kidney disease, Int. J. Biol. Sci. 14 (11) (2018) 1545–1557.
[29] W. Hou, B. Liu, H. Xu, Triptolide: medicinal chemistry, chemical biology and clinical progress, Eur. J. Med. Chem. 176 (2019) 378–392.
[30] J. Li, J. Jin, M. Li, C. Guan, W. Wang, S. Zhu, Y. Qiu, M. Huang, Z. Huang, Role of Nrf2 in protection against triptolide-induced toxicity in rat kidney cells, Toxicol. Lett. 213 (2) (2012) 194–202.
[31] W. Wang, G.D. Yao, X.Y. Shang, Y.Y. Zhang, X.Y. Song, T. Hayashi, Y. Zhang, S.J. Song, Eclalbasaponin I causes mitophagy to repress oxidative stress-induced apoptosis via activation of p38 and ERK in SH-SY5Y cells, Free Radic. Res. (2019) 1–14.
[32] T. Bell, Z. Hou, Y. Luo, M. Drew, E. Chapoteau, B. Czech, Kumar, Detection of creatinine by a designed receptor, Science 269 (5224) (1995) 671–674.
[33] N. Baum, C.C. Dichoso, C.E. Carlton, Blood urea nitrogen and serum creatinine, Urology 5 (5) (1975) 583–588.
[34] Blood urea nitrogen, in: A.L. Baert (Ed.), Encyclopedia of Diagnostic Imaging, Springer, Berlin Heidelberg, Berlin, Heidelberg, 2008, pp. 147–148.
[35] A. Andres-Hernando, N. Li, C. Cicerchi, S. Inaba, W. Chen, C. Roncal-Jimenez, M.T. Le, M.F. Wempe, T. Milagres, T. Ishimoto, M. Fini, T. Nakagawa, R.J. Johnson, M.A. Lanaspa, Protective role of fructokinase blockade in the pathogenesis of acute kidney injury in mice, Nat. Commun. 8 (2017) 14181.
[36] L.M. Shelton, B.K. Park, I.M. Copple, Role of Nrf2 in protection against acute kidney injury, Kidney Int. 84 (6) (2013) 1090–1095.
[37] E.W. Cloer, D. Goldfarb, T.P. Schrank, B.E. Weissman, M.B. Major, NRF2 activation in cancer: from DNA to protein, Cancer Res. 79 (5) (2019) 889–898.
[38] T. Patinen, S. Adinolfi, C.C. Cortes, J. Harkonen, A. Jawahar Deen, A.L. Levonen, Regulation of stress signaling pathways by protein lipoxidation, Redox Biol. (2019) 101114.
[39] A. Cuadrado, A.I. Rojo, G. Wells, J.D. Hayes, S.P. Cousin, W.L. Rumsey, O.C. Attucks, S. Franklin, A.-L. Levonen, T.W. Kensler, A.T. Dinkova-Kostova, Therapeutic targeting of the NRF2 and KEAP1 partnership in chronic diseases, Nat. Rev. Drug Discov. 18 (4) (2019) 295–317.
[40] S. Deller, P. Macheroux, S. Sollner, Flavin-dependent quinone reductases, Cell. Mol. Life Sci. 65 (1) (2008) 141–160.
[41] A.T. Dinkova-Kostova, P. Talalay, NAD(P)H:quinone acceptor oxidoreductase 1 (NQO1), a multifunctional antioxidant enzyme and exceptionally versatile cytoprotector, Arch. Biochem. Biophys. 501 (1) (2010) 116–123.
[42] K. Zhang, D. Chen, K. Ma, X. Wu, H. Hao, S. Jiang, NAD(P)H:quinone oxidoreductase 1 (NQO1) as a therapeutic and diagnostic target in cancer, J. Med. Chem. 61 (16) (2018) 6983–7003.
[43] A. Loboda, M. Damulewicz, E. Pyza, A. Jozkowicz, J. Dulak, Role of Nrf2/HO-1 system in development, oxidative stress response and diseases: an evolutionarily conserved mechanism, Cell. Mol. Life Sci. 73 (17) (2016) 3221–3247.
[44] R. Motterlini, R. Foresti, Heme oxygenase-1 as a target for drug discovery, Antioxid. Redox Signal. 20 (11) (2014) 1810–1826.
[45] V. Rubio, J. Zhang, M. Valverde, E. Rojas, Z.Z. Shi, Essential role of Nrf2 in protection against hydroquinone- and benzoquinone-induced cytotoxicity, Toxicol. In Vitro 25 (2) (2011) 521–529.
[46] R. Srividhya, V. Jyothilakshmi, K. Arulmathi, V. Senthilkumaran, P. Kalaiselvi, Attenuation of senescence-induced oxidative exacerbations in aged rat brain by (-)-epigallocatechin-3-gallate, Int. J. Dev. Neurosci. 26 (2) (2008) 217–223.